


Article

The Influence of Backwater Al^{3+} on Diaspore Bauxite Flotation

Chaojun Fang ¹, Ziyong Chang ², Qiming Feng ¹, Wei Xiao ¹ , Shichao Yu ¹, Guanzhou Qiu ¹ and Jun Wang ^{1,*}

¹ School of Minerals Processing & Bioengineering, Central South University, Changsha 410083, China; fangchaojun1009@126.com (C.F.); qmfeng@126.com (Q.F.); xiaowei2015@yahoo.com (W.X.); yushichao@csu.edu.cn (S.Y.); qgz@csu.edu.cn (G.Q.)

² School of Chemical Engineering, the University of Queensland, St Lucia, QLD 4072, Brisbane, Australia; z.chang@uq.edu.au

* Correspondence: wjwq2000@126.com; Tel.: +86-731-8887-6557

Received: 29 August 2017; Accepted: 10 October 2017; Published: 15 October 2017

Abstract: The effect of Al^{3+} in backwater on the flotation of diaspore bauxite was investigated by micro-flotation tests and the underlying mechanisms were investigated by inductively coupled plasma (ICP) measurement, zeta potential measurements, solution chemistry analyses, and synchrotron near edge X-ray absorption fine structure (NEXAFS) analyses. The ICP measurement results show the concentration of Al^{3+} in backwater was up to 1×10^{-4} mol/L. The micro-flotation results indicated that backwater Al^{3+} reduced the flotation recovery of diaspore and improved the flotation recovery of kaolinite at pH 9, which was the pH value used in the industrial flotation. The adsorption of Al^{3+} species changed the zeta potential, the Al atomic abundance, and the number of active sites on the mineral surface. In particular, the result of solution chemistry analyses and synchrotron NEXAFS analyses show that the Al^{3+} in backwater was adsorbed on the mineral surface in the form of $\text{Al}(\text{OH})_3$ (s), and the bond of $-\text{Al}-\text{O}-\text{Al}-(\text{OH})_2$ or $-\text{Al}/\text{Si}-\text{O}-\text{Al}-(\text{OH})_2$ was formed at pH 9. It changed the intensity of hydrogen bond force between minerals and collectors, and resulted in the depression of diaspore flotation and the activation of kaolinite flotation. This study can be used to guide the application of backwater in the flotation of diaspore bauxite in industry.

Keywords: backwater; Al^{3+} ; diaspore; bauxite; flotation

1. Introduction

It was reported that, until 2015, the bauxite ore reserves in China was 4.71 billion tons [1], and the majority was diaspore bauxite. Diaspore bauxite is unsuitable for direct extraction of alumina with Bayer process due to the low ration of alumina to silica (A/S). In the past few decades, the Bayer-mineral processing method has been developed by Chinese researchers to make better use of diaspore bauxite ore. The industrial test was completed in Xiaoguan Henan, China in 1999 and a satisfactory result has been achieved. For the bauxite with A/S 5.9, the concentration with A/S 11.39, and the recovery of 86.45% were gained [2].

The molecular model of diaspore and kaolinite are shown in Figure 1 [3,4]. The Al atomic abundance (Al molecules divided by the total number of molecules on the mineral surface) of diaspore surface is higher than that of kaolinite surface according to the molecular model. Zhang [5] calculated the Al atomic abundance of diaspore and kaolinite surface through X-ray photoelectron spectroscopy (XPS) tests, and he found that the atomic abundance of Al of diaspore surface was 1.7 times higher of that of kaolinite surface. It was considered that the atomic abundance of Al on the mineral surface was key to bauxite flotation.

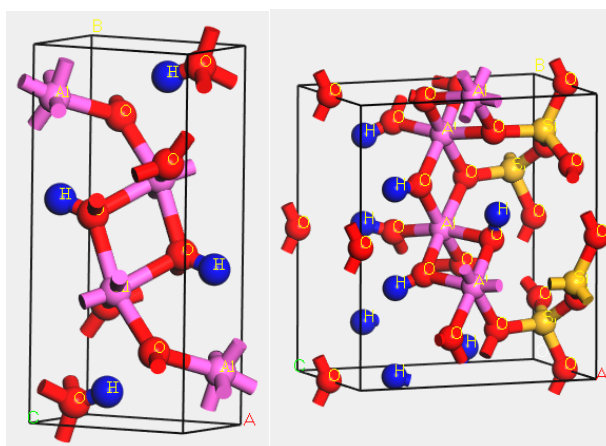


Figure 1. The molecular model of diaspore (left) and kaolinite (right).

The effects of metallic ions of mineral surface on mineral flotation have been extensively reported in literature [6–11]. Pb^{2+} species could interact with the iron-hydroxyl compounds, through chemisorption with the formation of a Fe–O–Pb complex on the ilmenite surface. As a result, the floatability of ilmenite can be improved by the addition of Pb^{2+} [12]. The flotation of hemimorphite could also be improved by Pb^{2+} species. Pb^{2+} was adsorbed on the hemimorphite through the compound of $\text{Pb}(\text{OH})_2$ (s), which promote the adsorption of NaOL and activated the flotation of hemimorphite [13]. Zn^{2+} species could inhibit the flotation of calcite by adsorbing on calcite surface with the formation of $\text{Zn}(\text{OH})_2$ (s), coating on the calcite surface, and inhibiting the interaction between the collectors and mineral surface [14]. Besides, Fe^{3+} could activate the flotation of spodumene, albite, quartz, which did not respond well to NaOL alone, by adsorbing on the mineral surface [15].

It was reported that backwater, the recycled water in the process of mineral processing, has a significant effect on the flotation of diaspore bauxite and some researchers had made effort to weaken the effect [16,17]. It was found that the organic acid was better to adjust the sedimentation condition than inorganic acid; it improved the quality of backwater and then weakened the adverse effect of backwater on the flotation of diaspore bauxite [16]. The quality of backwater also can be improved by the use of new flocculants, but the ratio of improved backwater should also be controlled at the suitable level to weaken the adverse effect of backwater on the flotation of diaspore bauxite [17]. However, the current research is limited about the effect of backwater metallic ions on the flotation of diaspore bauxite.

Due to the dissolution of bauxite and other reasons, a certain number of Al^{3+} will be presented in backwater and it would have an important effect on the flotation of bauxite. Diaspore and kaolinite were the most important minerals of diaspore bauxite [18] and were chosen as the research object. This paper will be helpful for further developing an approach to reduce the adverse effects of backwater Al^{3+} on the flotation of diaspore bauxite and finally to guide the industrial flotation.

2. Materials and Methods

2.1. Minerals

The minerals (diaspore and kaolinite) used in the experiments were taken from Xiaoyi, Shanxi province, China. The block minerals were hand-picked, crushed, and ground with a laboratory porcelain mill. After grinding, the milled minerals were wet-sieved with distilled water and divided into three different sizes. The particles with the size of $-0.074 + 0.038$ mm was used for flotation tests, while the particles with the size of -0.038 mm was used for Synchrotron NEXAFS analyses. A portion of the size under 0.038 mm was further ground to -5 μm with an agate mortar for zeta potential measurements.

The minerals were confirmed by Chemical composition analysis and X-ray diffraction (XRD) analyses. Table 1 shows the chemical compositions of diaspore and kaolinite samples. The alumina-silica ratios (A/S) of diaspore and kaolinite were 98.61 and 0.91, respectively. The XRD analyses results of diaspore (a) and kaolinite (b) samples are shown in Figure 2, which indicated that both diaspore and kaolinite were of high purity.

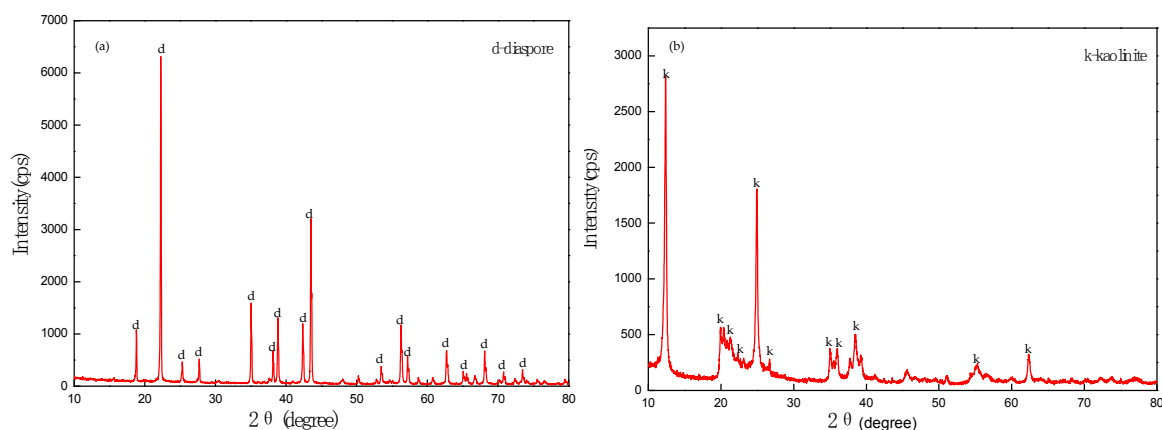


Figure 2. X-ray Diffraction (XRD) results of diaspore (a) and kaolinite (b).

Table 1. Mineral chemical composition analysis results (%).

Sample	Al ₂ O ₃	SiO ₂	Fe ₂ O ₃	TiO ₂	CaO	MgO	K ₂ O	Na ₂ O	LOI
Diaspore	80.86	0.82	0.24	2.81	0.01	0.049	0.008	0.029	14.62
Kaolinite	39.61	43.55	0.34	1.86	0.015	0.071	0.01	0.026	14.18

2.2. Reagents

Table 2 shows the ICP measurement results of metallic ions in fresh water and backwater. When used for industrial flotation, an additional 20% fresh water was usually added to backwater. Hence, the concentration of Al³⁺ in backwater was about 1×10^{-4} mol/L. There are other metallic ions, organic reagents, and superfine minerals existing in the backwater in addition to Al³⁺ ions, which may also influence the flotation behavior of diaspore bauxite. To study the influence of Al³⁺ on the flotation of diaspore and kaolinite, aluminium sulfate octadecahydrate (Al₂(SO₄)₃·18H₂O) was used as the substitutive source of backwater Al³⁺. Dilute hydrochloric acid (HCl) solution and dilute sodium hydroxide (NaOH) solution were used as pH regulators. Sodium oleate (NaOL) was used as the collector of the experiments with the concentration of 5×10^{-4} mol/L. The reagents used in the experiments were all of analytical purity. The distilled water was used throughout the whole experiments.

Table 2. Inductively coupled plasma (ICP) measurement results of backwater.

Sample	Ca ²⁺ (mmol/L)	Mg ²⁺ (mmol/L)	Al ³⁺ (mmol/L)	Fe ³⁺ (mmol/L)
Fresh water	1.793	0.838	0.004	0.018
Backwater	0.215	0.077	0.130	0.008

2.3. Micro-Flotation Tests

A XFG flotation machine (Jilin Exploration Machinery Factory, Changchun, China) with a volume of 40 mL and a stirring speed of 1650 rpm was used for the flotation tests. The flotation temperature was fixed at 25 ± 2 °C. The 2 g purified mineral particles and 38 mL distilled water were added into the flotation cell. After 1 min of stirring, pH regulators were added to control the solution pH

value in the predetermined range. Then, the prepared backwater Al^{3+} and NaOL solutions were successively added, and each reagent was conditioned for 2 min. The flotation was carried out for 3 min. The concentrate and tailing were separately filtered, dried, and collected. Finally, the recoveries were calculated.

2.4. Zeta Potential Measurements

A ZetaPALS instrument (Brookhaven Instruments Corporation, Brookhaven, NY, USA) was used to measure the zeta potential of the mineral surface. The suspension was prepared by adding 0.025 g mineral to 50 mL 0.01 mol/L KCl solution. Then pH regulators, backwater Al^{3+} , and NaOL solutions were added in order. The final suspension was stirred for 15 min while the pH was regulated within the predetermined range.

2.5. Synchrotron X-ray Absorption Spectroscopy Analyses

The C 1s and O 1s K-edge near edge X-ray absorption fine structure (NEXAFS) spectra were obtained on beamline 4B9B at the Beijing Synchrotron Radiation Facility (BSRF) located in the Institute of High Energy Physics, Chinese Academy of Science, Beijing, China. The spectra range of C K-edge NEXAFS was between 275 eV and 300 eV with the step of 0.1 eV, and the spectra range of O K-edge NEXAFS was between 525 eV and 560 eV with the step of 0.1 eV, respectively. The position of spectra were revised by Au standard sample. The normalization and background removal of C 1s NEXAFS spectra were completed by ATHENA 0.9.25 software (Demeter, Upton, NY, USA) [19]. The samples were conditioned with the same conditioning regime as the micro-flotation tests without the flotation process, the pH was conditioned at pH 9. Then, the samples were filtrated and rinsed by distill water in order to remove any weakly adsorbed particles. The prepared samples were dried in a vacuum oven at temperature for 24 h.

3. Results and Discussion

3.1. The Effects of Backwater Al^{3+} on Diaspore and Kaolinite Flotation Recoveries

Figure 3 presents the effect of Al^{3+} on the flotation recoveries of diaspore and kaolinite at different flotation pH. In the absence of Al^{3+} , the recovery of diaspore increased rapidly with an increase in pH until a maximum recovery about 95% was achieved at pH 8, and then the flotation recovery tended to remain stable with the further addition of dilute sodium hydroxide. While in presence of Al^{3+} , the recovery of diaspore decreased gradually with an increase in pH until a recovery about 50% was obtained at pH 9. After that, the recovery rose rapidly with an increase in pH and a recovery about 95% was obtained at pH above 10. It indicated that Al^{3+} activated the flotation of diaspore in acidic condition and intensely inhibited the flotation of diaspore in weak alkaline condition. Especially, Al^{3+} decreased the recovery of diaspore from 95% to 50% at pH 9, the pH value commonly used in industrial flotation. Meanwhile, Figure 3 shows that in the absence of Al^{3+} , the recovery of kaolinite firstly increased gradually with an increase in pH, and a recovery of about 27% was obtained at pH 7, and then the flotation recovery decreased sharply to 0.05% at pH 9. While in the presence of Al^{3+} , the recovery had a slight increase in acidic condition and a significant increase at pH 7–10. In particular, the recovery of kaolinite almost approached the recovery of diaspore at pH 9, the pH value commonly used in industrial flotation.

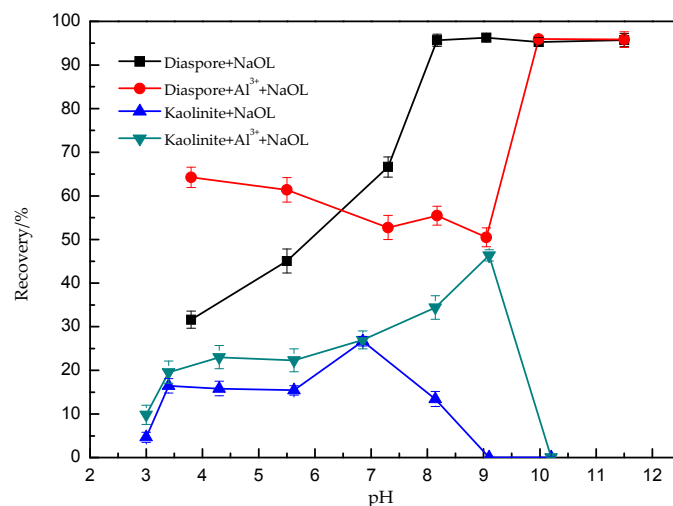


Figure 3. Flotation recoveries of diaspore and kaolinite with and without backwater Al^{3+} (Al^{3+} : 1×10^{-4} mol/L; Sodium oleate (NaOL): 5×10^{-4} mol/L).

The results suggested that with the adsorption of backwater Al^{3+} species, the flotation of diaspore was strongly inhibited while the flotation of kaolinite was strongly activated.

3.2. Solution Chemistry Analyses

In general, the metallic ion may adsorb on the mineral surface by electrostatic forces, by the formation of monohydric compound, or by hydroxide compound. When investigating the effect of metallic ions on the flotation of quartz and beryl, Fuerstenau [20] found that the best pH value of flotation was in accord with the pH value of maximum content of monohydric compound, and then the monohydric compound adsorption type was established. Besides, the hydroxide compound adsorption type was established by Wang [21] according to the solution chemistry theory.

The concentration logarithmic diagrams of backwater Al^{3+} and NaOL was calculated by the solution chemistry theory with the initial concentration of 1×10^{-4} mol/L and 5×10^{-4} mol/L, respectively. The results are shown in Figures 4 and 5. According to Figure 4, the main species of Al^{3+} are Al^{3+} below pH 4, Al^{3+} and $\text{Al}(\text{OH})_2^+$ near pH 4, $\text{Al}(\text{OH})_3(\text{s})$ between pH 6–9, and $\text{Al}(\text{OH})_4^-$ above pH 10, respectively. Figure 5 indicates that $\text{H}(\text{OL})_2^-$, considered to be the most effective species of NaOL [21], which has a higher concentration near pH 9 relative to other pH.

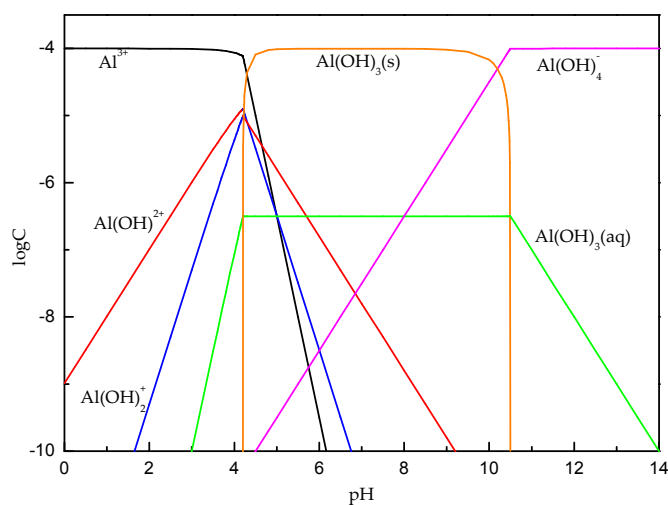


Figure 4. Concentration logarithmic diagram of backwater Al^{3+} (Al^{3+} : 1×10^{-4} mol/L).

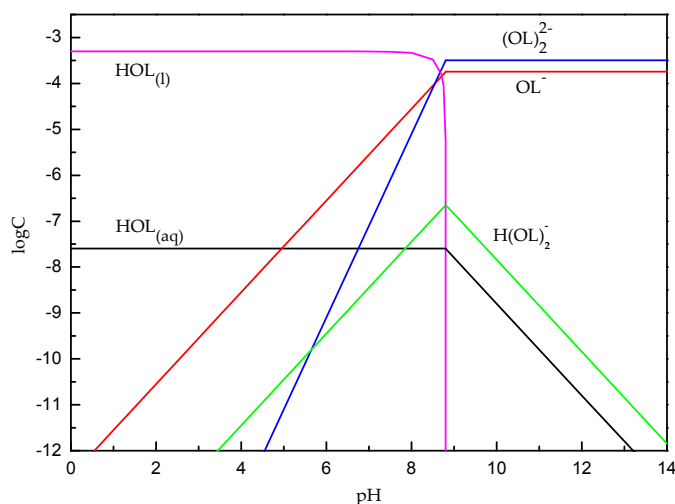


Figure 5. Concentration logarithmic diagram of NaOL (NaOL: 5×10^{-4} mol/L).

Figures 4 and 5 are helpful in explaining the flotation recovery of diaspore and kaolinite. Due to the adsorption of Al^{3+} and $\text{Al}(\text{OH})^{2+}$ at pH 4, the mineral surface is positively charged, which can facilitate the adsorption of OL^- on mineral surface by the electrostatic attraction. As a result, the recovery of diaspore and kaolinite at pH 4 in presence of Al^{3+} species was higher than that in absence of Al^{3+} species. At pH 7–9, the main species of Al^{3+} was $\text{Al}(\text{OH})_3$ (s), which coated on the diaspore surface and prevented the directly interaction between mineral and collector, resulting in the decrease of flotation recovery. At pH higher than 10, as the generation of $\text{Al}(\text{OH})_4^-$ instead of $\text{Al}(\text{OH})_3$ (s), collector renewed the direct interaction with the mineral surface, and the flotation recovery increased. As for the flotation of kaolinite, the number of active sites with collector increased with the adsorption of $\text{Al}(\text{OH})_3$ (s) at pH 9. Besides, the concentration of $\text{H}(\text{OL})_2^-$ reached a high level at pH 9, both resulting in the highest recovery of kaolinite. When pH was higher than 10, the flotation recovery decreased significantly due to the reduction of $\text{Al}(\text{OH})_3$ (s) and $\text{H}(\text{OL})_2^-$.

It is worth noting that the recovery of kaolinite almost approached the recovery of diaspore at pH 9, the probable reason was that $\text{Al}(\text{OH})_3$ (s) was unselectively adsorbed on the diaspore and kaolinite surface, greatly reducing the difference between the two mineral surfaces and then leading to the similar flotation recovery.

3.3. Zeta Potential Measurements

The pH value has an important influence on zeta potential [22]. The adsorption of metallic ions on the mineral surface would lead to the variation in the zeta potential of mineral surface and alter the isoelectric point (IEP) [23–29]. The adsorption of cationic or anionic collectors has similar effects [30–33].

Figure 6 presents the zeta potential of diaspore under four different treatments. In the absence of backwater Al^{3+} and NaOL, the zeta potential of diaspore decreased with an increase in pH and the IEP of diaspore was 4.6. However, the zeta potential of diaspore increased obviously with the addition of backwater Al^{3+} , and the IEP of diaspore was shifted from 4.6 to 6.5. It indicated that backwater Al^{3+} was adsorbed on the mineral surface and changed the zeta potential. When diaspore was treated with NaOL alone, there was a significant decrease of zeta potential of diaspore due to the strongly adsorption of NaOL. Besides, the zeta potential of diaspore decreased sharply in neutral condition and alkaline condition in the presence of backwater Al^{3+} and NaOL.

When combining with Figures 3 and 4, backwater Al^{3+} mainly exist in the species of Al^{3+} and $\text{Al}(\text{OH})^{2+}$ near pH 4, though Al^{3+} would react with NaOL and decreased the concentration of NaOL, the interaction between mineral surface and collector was intensified due to the adsorption of $\text{Al}(\text{OH})^{2+}$,

which resulted in a higher flotation recovery. Meanwhile, Al^{3+} mainly exist in the species of $\text{Al}(\text{OH})_3$ (s) at pH 7–9, which was adsorbed on the diaspore surface and had a small effect on zeta potential, but the direct interaction between mineral surface and collector was prevented, resulting in the decrease of the flotation recovery. However, the main species of Al^{3+} was $\text{Al}(\text{OH})_4^-$ above pH 10, which was not adsorbed on the diaspore surface and almost had no effect on zeta potential according to Figure 6, but it renewed the direct interaction between mineral surface and collector, and finally increased the flotation of diaspore.

Figure 7 shows the results of zeta potential measurement of kaolinite under four different treatments. The natural IEP of kaolinite was 3.6, but with the addition of backwater Al^{3+} , the IEP of kaolinite was shifted to 6.8. In addition, it is worth noting that the highest zeta potential appeared at pH 4, it can be speculated that backwater Al^{3+} was adsorbed on the kaolinite surface in the species of $\text{Al}(\text{OH})^{2+}$, according to Figure 4, which was consistent with the reports of Fuerstenau [20]. When treated with NaOL alone, the zeta potential of kaolinite was decreased due to the adsorption of NaOL. However, in the presence of backwater Al^{3+} and NaOL, the zeta potential was lower than that of treated with NaOL alone at pH 7–9. When combining with Figures 3 and 4, it can be known that Al^{3+} mainly exist in the species of $\text{Al}(\text{OH})_3$ (s) at pH 7–9, which increased the number of active sites and the adsorption of collector, decreased the zeta potential and improved the flotation of kaolinite.

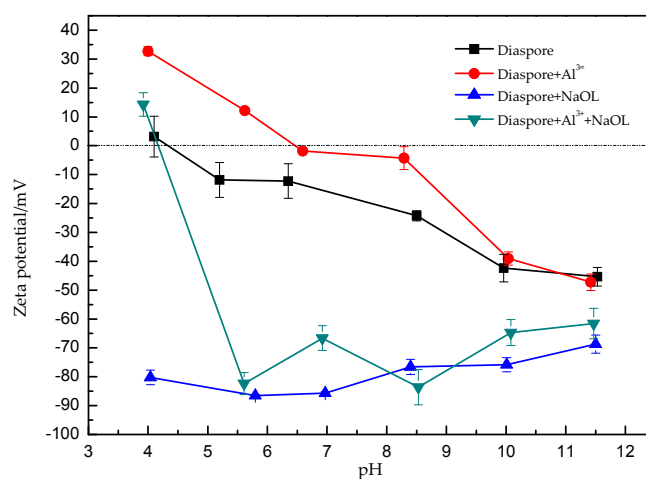


Figure 6. Zeta potential of diaspore under four different treatments (Al^{3+} : 1×10^{-4} mol/L; NaOL: 5×10^{-4} mol/L).

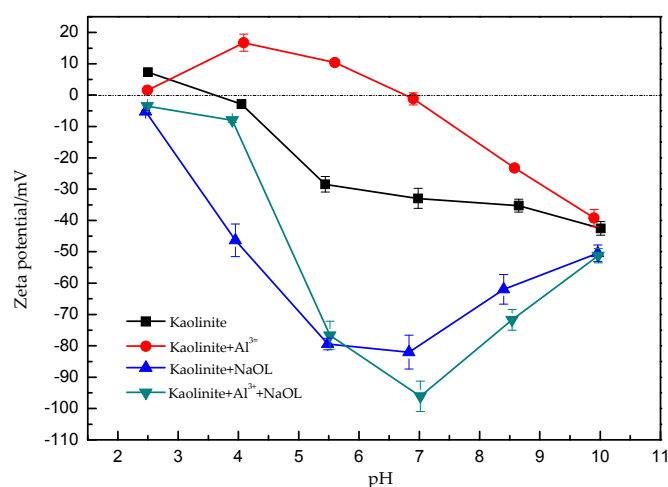


Figure 7. Zeta potential of kaolinite under four different treatments (Al^{3+} : 1×10^{-4} mol/L; NaOL: 5×10^{-4} mol/L).

3.4. Synchrotron X-ray Absorption Spectroscopy Analyses

Figures 8 and 9 show the C 1s and O 1s NEXAFS spectra of diaspore and kaolinite at pH 9, respectively. The NEXAFS spectra presented the fine changes in chemical environment of chemical elements. Hence, C and O K-edge X-ray absorption spectroscopy was used to investigate some important issues such as graphene, nano-materials, life science, medical science, and catalysts [34–44].

The sole source of C was NaOL in the NEXAFS analyses. Some approximate energy ranges and primary absorption peaks of C 1s NEXAFS were listed in Table 3 [45]. According to Figure 8, there were four C K-edge absorption peaks of diaspore when NaOL was added alone. The peak positions were 285.0 eV, 287.5 eV, 288.6 eV, 289.7 eV, representing the bond of C=C, C–H, R–COOH, COO[−], respectively. When backwater Al³⁺ was added with NaOL, the peak positions at 288.6 eV and 289.7 eV had no change but the proportion of absorption regions were decreased. It indicated that the adsorption of HOL and OL[−] decreased due to the presence of backwater Al³⁺ species.

The C K-edge X-ray absorption spectra of kaolinite was different from that of diaspore. When kaolinite was conditioned with NaOL alone, there were three absorption peaks located at 284.9 eV, 288.1 eV, 290.0 eV, which represented the bond of C=C, R–COOH, COO[−], respectively. With the addition of backwater Al³⁺ and NaOL, the peak positions had no change, only the proportion of peak at 288.1 eV decreased. It suggested that in the presence of backwater Al³⁺ species, the adsorption of HOL decreased but the adsorption of OL[−] almost had no change, indicating that OL[−] was the more important species of NaOL at pH 9.

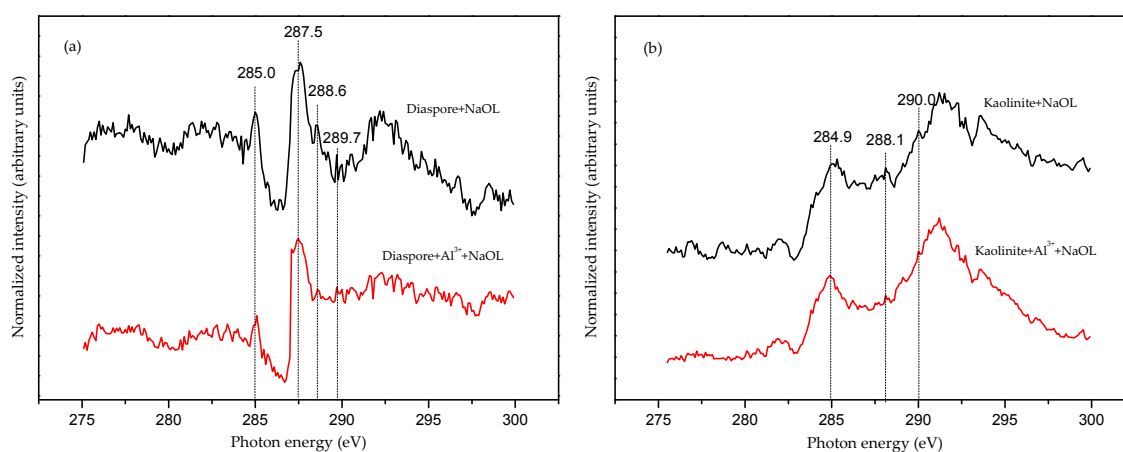


Figure 8. C 1s Near Edge X-ray Absorption Fine Structure (NEXAFS) total electron yield spectra of: (a) diaspore and (b) kaolinite (pH = 9).

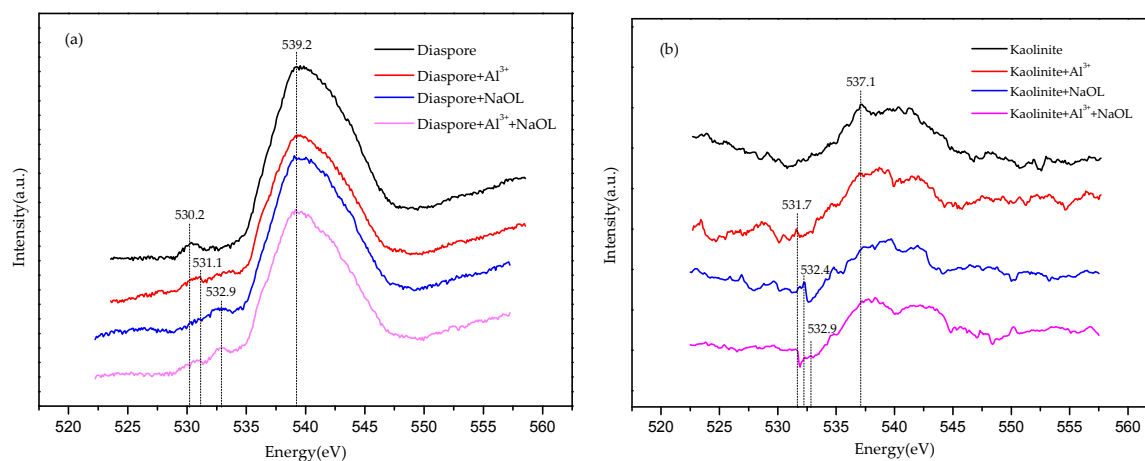


Figure 9. O 1s NEXAFS total electron yield spectra of: (a) diaspore and (b) kaolinite (pH = 9).

Table 3. C 1s NEXAFS approximate energy ranges and primary absorption peaks [45].

C Form	Bond	Peak Energy (eV)	Fit Position (eV)
Aromatic C	C=O	283–284.5	284.5
Aromatic C	C=C	284.9–285.5	285.4
Alkyl C	C–H	287–287.6	287.6
Carboxylic C	R–COOH	288–288.7	288.4
O-alkyl C/carbonyl	COO [−]	289.5–290.2	289.9

The NEXAFS of O was more complex than C. On one hand, there were O elements on the mineral crystal and surface. On the other hand, water, O₂ and NaOL would bring new O source to the mineral surface. Figure 9a shows that without the addition of backwater Al³⁺ and NaOL, there were two absorption peaks of diaspore at 530.2 eV and 539.2 eV. With the addition of backwater Al³⁺ alone, the peak at 530.2 eV was shifted to 531.1 eV, which indicated that the form of O was changed from –Al–O–H to –Al–O–Al–(OH)₂ due to the adsorption of backwater Al³⁺ species.

When NaOL was added alone, the peak at 530.2 eV was shifted to 532.9 eV. Because the major interaction between the mineral surface and collector was hydrogen bonding [5]. The form of O may change from –Al–O–H to –Al–O–H···RCOO[−] (“···” means Hydrogen bond). In the presence of backwater Al³⁺ and NaOL, two absorption peaks appeared at 531.1 eV and 532.9 eV, which represented the O form of –Al–O–Al–(OH)₂ and –Al–O–Al–(OH)₂···RCOO[−]. In addition, the intensity of the peak at 532.9 eV was lower than that in absence of backwater Al³⁺ species. Therefore, it suggested that with the addition of backwater Al³⁺, the O form of diaspore surface firstly transformed from –Al–O–H to –Al–O–Al–(OH)₂, and then with the addition of NaOL, the hydrogen bond of –Al–O–Al–(OH)₂···RCOO[−] existed instead of –Al–O–H···RCOO[−]. Because the hydrogen bond force of –Al–O–H···RCOO[−] was stronger than –Al–O–Al–(OH)₂···RCOO[−]. It can be concluded that backwater Al³⁺ decreased the interaction between the diaspore surface and collector, resulting in the depression of diaspore flotation.

As shown in Figure 9b, there was no absorption peak of kaolinite at 530.2 eV in the absence of Al³⁺ and NaOL, which indicated that there was rare –Al–O–H on the kaolinite surface. In the presence of backwater Al³⁺ alone, a new peak appeared at 531.7 eV, indicating that backwater Al³⁺ species was adsorbed on the kaolinite surface and formed a new bond –Al/Si–O–Al–(OH)₂. When NaOL was added alone, there appeared a new peak at 532.4 eV, indicating the adsorption of NaOL and the formation of –Al/Si–O–H···RCOO[−]. In the presence of backwater Al³⁺ and NaOL, the new peak at 532.4 eV was shifted to 532.9 eV, representing the O form of –Al/Si–O–Al–(OH)₂···RCOO[−]. Therefore it suggested that with the addition of backwater Al³⁺, the O form of –Al/Si–O–Al–(OH)₂ firstly appeared on kaolinite surface, and then the hydrogen bond of –Al/Si–O–Al–(OH)₂···RCOO[−] formed with the addition of NaOL. Because the hydrogen bond force of –Al/Si–O–Al–(OH)₂···RCOO[−] was stronger than –Al/Si–O–H···RCOO[−], hence, it can be concluded that backwater Al³⁺ increased the interaction between the kaolinite surface and collector, resulting in the activation of diaspore flotation at pH 9.

Hence, when combining the result of O 1s NEXAFS analyses and the flotation system, the approximate energy ranges and primary absorption peaks of O 1s NEXAFS of diaspore and kaolinite surface were established in Table 4.

Table 4. O 1s NEXAFS approximate energy ranges and primary absorption peaks (“...” means Hydrogen bond).

O Form	Bond	Peak Energy (eV)	Fit Position (eV)
–Al–O–H	–Al–O–H	529.6–530.6	530.2
–Al–O–Al–(OH) ₂	–Al–(OH) ₂	530.7–531.2	531.1
–Al/Si–O–Al–(OH) ₂	–Al–(OH) ₂	531.3–531.9	531.7
–Al/Si–O–H...RCOO [−]	–Al/Si–O–H...O	532.0–532.4	532.4
–Al–O–H...RCOO [−]	–Al–O–H...O	532.5–533.8	532.9
–Al–O–Al–(OH) ₂ ...RCOO [−]	–Al–O–H...O	532.5–533.3	532.9
–Al/Si–O–Al–(OH) ₂ ...RCOO [−]	–Al–O–H...O	532.5–533.0	532.9

4. Conclusions

In this paper, the influence of backwater Al³⁺ on the flotation of diaspore bauxite was studied and the underlying mechanisms were investigated. It was found that backwater Al³⁺ inhibited the flotation of diaspore while it activated the flotation of kaolinite at pH 9.

The zeta potential was increased and the IEP was shifted with the adsorption of backwater Al³⁺. At pH 9, backwater Al³⁺ was adsorbed on diaspore and kaolinite surface in the species of Al(OH)₃ (s), which changed the Al atomic abundance and the active sites of diaspore and kaolinite. Besides, the bond of –Al–O–Al–(OH)₂ or –Al/Si–O–Al–(OH)₂ was formed due to the adsorption of Al(OH)₃ (s), which decreased the hydrogen bond force between diaspore surface and collector while it increased the hydrogen bond force between kaolinite surface and collector. Finally, it resulted in the inhibition of diaspore flotation and the activation of kaolinite flotation.

Acknowledgments: Authors acknowledge the financial support of the National Natural Science Foundation of China (No. 51474254), and China Postdoctoral Science Foundation (No. 2013M531813). We are grateful to the staff at beamline 4B9B and other professors of Beijing Synchrotron Radiation Facility (BSRF) for their help in beamline operation, data collection and direction.

Author Contributions: Chaojun Fang, Qiming Feng, Guanzhou Qiu and Jun Wang conceived and designed the experiments; Chaojun Fang, Shichao Yu and Jun Wang prepared the samples, performed the experiments and analyzed the data. Chaojun Fang, Ziyong Chang, Wei Xiao and Jun Wang contributed to the writing and revising of the paper.

Conflicts of Interest: The authors declare no conflict of interest.

References

1. Wang, M.; Peng, Q.M. Chapter 1, China Mineral Resources. In *Situation of Mineral Resources*; Geological Publishing House: Beijing, China, 2016; p. 5.
2. Aluminum Corporation of China Limited; Beijing General Research Institute of Mining & Metallurgy; Central South University of Technology. *Total Report of Bayer-Mineral Processing Method Producing Alumina*; China Nonferrous Metals Industry Association: Beijing, China, 1999.
3. Friedrich, A.; Wilson, D.J.; Haussuhl, E.; Winkler, B.; Morgenroth, W.; Refson, K.; Milman, V. High-pressure properties of diaspore, AlO(OH). *Phys. Chem. Miner.* **2007**, *34*, 145–157. [[CrossRef](#)]
4. Bish, D.L. Rietveld refinement of the kaolinite structure at 1.5 K. *Clays Clay Miner.* **1993**, *41*, 738–744. [[CrossRef](#)]
5. Zhang, G.F. Theory and Technology of Flotation on Bauxite Desilicate. Ph.D. Thesis, Central South University, Changsha, China, 2001.
6. Fatai, I.; Maria, M.; Bjorn, J.; Kota, H.R. Recycling of process water in sulphide flotation: Effect of calcium and sulphate ions on flotation of galena. *Miner. Eng.* **2012**, *39*, 77–88.
7. Morkel, J.; Pistorius, P.C.; Vermaak, M.K.G. Cation exchange behavior of kimberlite in solutions containing Cu²⁺ and K⁺. *Miner. Eng.* **2007**, *20*, 1145–1152. [[CrossRef](#)]
8. Costa, C.A.; Rubio, J. Deinking flotation: Influence of calcium soap and surface-active substances. *Miner. Eng.* **2005**, *18*, 59–64. [[CrossRef](#)]

9. Kirjavainen, V.; Schreithofer, N.; Heiskanen, K. Effect of calcium and thiosulfate ions on flotation selectivity of nickel-copper ores. *Miner. Eng.* **2002**, *15*, 1–5. [[CrossRef](#)]
10. Liu, R.Q.; Guo, Y.Z.; Wang, L.; Sun, W.; Tao, H.B.; Hu, Y.H. Effect of calcium hypochlorite on the flotation separation of galena and jamesonite in high-alkali systems. *Miner. Eng.* **2015**, *84*, 8–14. [[CrossRef](#)]
11. Gan, W.B.; Brendan, C.; Liu, Q. Effect of citric acid on inhibiting hexadecane-quartz coagulation in aqueous solutions containing Ca^{2+} , Mg^{2+} and Fe^{3+} ions. *Int. J. Miner. Process.* **2009**, *92*, 84–91. [[CrossRef](#)]
12. Chen, P.; Zhai, J.H.; Sun, W.; Hu, Y.H.; Yin, Z.G.; Lai, X.S. Adsorption mechanism of lead ions at ilmenite/water interface and its influence on ilmenite flotability. *J. Ind. Eng. Chem.* **2017**, *53*, 285–293. [[CrossRef](#)]
13. Liu, C.; Feng, Q.M.; Zhang, G.F.; Ma, W.K.; Meng, Q.Y.; Chen, Y.F. Effects of lead ions on the flotation of hemimorphite using sodium oleate. *Miner. Eng.* **2016**, *8*, 163–167. [[CrossRef](#)]
14. Shi, Q.; Zhang, G.F.; Feng, Q.M.; Ou, L.M.; Lu, Y.P. Effect of the lattice ions on the calcite flotation in presence of Zn(II). *Miner. Eng.* **2013**, *40*, 24–29. [[CrossRef](#)]
15. Zhang, J.; Wang, W.Q.; Liu, J.; Huang, Y.; Feng, Q.M.; Zhao, H. Fe(III) as an activator for the flotation of spodumene, albite, and quartz minerals. *Miner. Eng.* **2014**, *61*, 16–22.
16. Jiang, Y.Q. Research on Dewatering and Water Recycling for Bauxite Direct-Flotation Tailings. Master's Thesis, Central South University, Changsha, China, 2011.
17. He, P.B.; Liu, H.; Chen, X.H. Influence of backwater on bauxite flotation desilication. *Nonferr. Met.* **2011**, *3*, 25–28.
18. Ou, L.M.; Feng, Q.M.; Chen, Y.; Lu, Y.P.; Zhang, G.F. Disintegration mode of bauxite and selective separation of Al and Si. *Miner. Eng.* **2006**, *20*, 200–203. [[CrossRef](#)]
19. Ravel, B.; Newville, M. ATHENA, ARTEMIS, HEPHAESTUS: Data analysis for X-ray absorption spectroscopy using IFEFFIT. *J. Synchrotron Radiat.* **2005**, *12*, 537–541. [[CrossRef](#)] [[PubMed](#)]
20. Fuerstenau, M.C. *Flotation: A. M. Gaudin Memorial Volume*; American Institute of Mining, Metallurgical, and Petroleum Engineers, Inc.: New York, NY, USA, 1976; Volume 1, pp. 148–150.
21. Wang, D.Z.; Hu, Y.H. *Solution Chemistry of Flotation*; Hunan Science and Technology Press: Changsha, China, 1988; Volume 6, pp. 132–179.
22. Fuerstenau, D.W.; Pradip. Zeta potentials in the flotation of oxide and silicate minerals. *Adv. Colloid Interface Sci.* **2005**, *114–115*, 9–26. [[CrossRef](#)] [[PubMed](#)]
23. Zhou, Y.L.; Hu, Y.H.; Wang, Y.H. Effect of metallic ions on dispersibility of diasporite. *Trans. Nonferr. Met. Soc. China* **2011**, *21*, 1166–1171. [[CrossRef](#)]
24. Peng, H.Q.; Luo, W.; Wu, D.; Bie, X.X.; Shao, H.; Jiao, W.Y.; Liu, Y.K. Study on the effect of Fe^{3+} on zircon flotation separation from cassiterite using sodium oleate as collector. *Minerals* **2017**, *7*, 108. [[CrossRef](#)]
25. Xiao, W.; Cao, P.; Liang, Q.N.; Peng, H.; Zhao, H.B.; Qin, W.Q.; Qiu, G.Z.; Wang, J. The activation mechanism of Bi^{3+} ions to rutile flotation in a strong acidic environment. *Minerals* **2017**, *7*, 113. [[CrossRef](#)]
26. Li, F.X.; Zhong, H.; Wang, S.; Liu, G.Y. The activation mechanism of Cu(II) to ilmenite and subsequent flotation response to α -hydroxyoctyl phosphinic acid. *J. Ind. Eng. Chem.* **2016**, *37*, 123–130. [[CrossRef](#)]
27. Jiang, H. Studies on Solution Chemistry of Interactions between Cationic Collectors and Aluminosilicate Aluminum Minerals in Bauxite Flotation Desilica. Ph.D. Thesis, Central South University, Changsha, China, 2004.
28. Lu, Y.P. Research on Bauxite Desilication by Selective Grinding-Aggregation Flotation. Ph.D. Thesis, Central South University, Changsha, China, 2012.
29. Zhou, Y.L. Investigation of the Influence of Metal Ions on Selective Dispersion of Diasporite and Silicate Minerals. Ph.D. Thesis, Central South University, Changsha, China, 2011.
30. Wang, J.; Cheng, H.W.; Zhao, H.B.; Qin, W.Q.; Qiu, G.Z. Flotation behavior and mechanism of rutile with nonyl hydroxamic acid. *Rare Metals* **2016**, *35*, 419–424. [[CrossRef](#)]
31. Gao, Z.Y.; Sun, W.; Hu, Y.H. New insights into the dodecylamine adsorption on scheelite and calcite: An adsorption model. *Miner. Eng.* **2015**, *79*, 54–61. [[CrossRef](#)]
32. Gao, Z.Y.; Bai, D.; Sun, W.; Cao, X.F.; Hu, Y.H. Selective flotation of scheelite from calcite and fluorite using a collector mixture. *Miner. Eng.* **2015**, *72*, 23–26. [[CrossRef](#)]
33. Gao, Y.S.; Gao, Z.Y.; Sun, W.; Hu, Y.H. Selective flotation of scheelite from calcite: A novel reagent scheme. *Int. J. Miner. Process.* **2016**, *154*, 10–15. [[CrossRef](#)]

34. Christopher, E.; Wolfgang, E.S.U.; Peter, S. C K-edge NEXAFS spectra of graphene with physical and chemical defects: A study based on density functional theory. *Phys. Chem. Chem. Phys.* **2014**, *16*, 14083.
35. Mikael, T.; Rainer, B.; Karina, T.; Chithra, K.; Ulf, S.; Torbjorn, A.L. Nanomapping and speciation of C and Ca in thermally treated lignocellulosic cell walls using scanning transmission X-ray microscopy and K-edge XANES. *Fuel* **2016**, *167*, 149–157.
36. Akihito, I.; Hidenori, S.; Naomichi, O.; Hiroshi, K.; Toshiaki, O.; Yoshihiro, N. Pretreatment Dependence of Adsorption Properties of Merocyanine Dye at Rutile (110) and 100 TiO₂ surface study by C K-edge NEXAFS. *J. Phys. Chem. C* **2009**, *113*, 17254–17261.
37. Francesca, G.; Paola, Z.; Alain, J.C.; Marco, N.; Enrico, T.; Davide, B.; Maria, G.P. Stability and extreme ultraviolet photo-reduction of graphene during C-K-edge characteraction. *Surf. Coat. Technol.* **2016**, *296*, 211–215.
38. Alberto, B.; Marco, M.; Vincenzo, B.; Giovanna, F.; Gustavo, A.C.J.; Mauro, S.; Cesare, G.; de Monica, S.; Marcello, C. Vibrationally resolved NEXAFS at C and N K-edges of pyridine, 2-fluoropyridine and 2,6-difluoropyridine: A combined experimental and theoretical assessment. *J. Chem. Phys.* **2015**, *143*, 204102.
39. Masaaki, Y.; Yosuke, M.; Takehiro, M.; Masanari, N.; Hayato, Y.; Nobuhiro, K.; Hiroshi, K. Direct Observation of Active Nickel Oxide Cluster in Nickel–Borate electrocatalyst for water oxidation by in situ O K-edge X-ray absorption spectroscopy. *J. Phys. Chem. C* **2015**, *119*, 19279–19286.
40. Natalia, P.; Anil, A.; Teguh, C.A.; Diao, C.Z.; Yu, X.J.; Mark, B.H.B.; Venkatesan, T.; Ariando; Andriwo, R. Electronic defect states at the LaAlO₃/SrTiO₃ heterointerface revealed by O K-edge X-ray absorption spectroscopy. *Phys. Chem. Chem. Phys.* **2016**, *18*, 13844.
41. Benjamin, J.A.M.; Grant, S.H.; Hiroshi, F.; Nozomu, H.; de Dominique, L.; Camille, S.; Masami, K. In situ structural changes of amorphous diopside (CaMgSi₂O₆) up to 20 GPa: A Raman and O K-edge X-ray Roman spectroscopic study. *Geochim. Cosmochim. Acta* **2016**, *178*, 41–61.
42. Guglieri, C.; Chaboy, J. O K-Edge X-ray Absorption Spectroscopy in Al-Doped ZnO Materials: Structural vs Electronic Effects. *J. Phys. Chem.* **2014**, *118*, 25779–25785. [[CrossRef](#)]
43. Liu, X.; Dean, M.P.; Liu, J.; Chluzbalan, S.G.; Jaouen, N.; Nicolaou, A.; Yin, W.G.; Rayan Serrao, C.; Ramesh, R.; Ding, H.; et al. Probing single magnon excitations in Sr₂IrO₄ using O K-edge resonant inelastic X-ray scattering. *J. Phys. Condens. Matter* **2015**, *27*, 202202. [[CrossRef](#)] [[PubMed](#)]
44. Benjamin, J.A.M.; Grant, S.H.; Camille, S.; Cedrick, O.S.; Lucia, Z.; Tom, R.; de Dominique, L. The structure of haplobasaltic glasses investigated using X-ray absorption near edge structure (XANES) spectroscopy at the Si, Al, Mg, and O K-edges and Ca, Si, and Al L_{2,3}-edges. *Chem. Geol.* **2016**, *420*, 213–230.
45. Karen, H.; Johannes, L.; Dawit, S.; Michael, W.I.S.; Thomas, R. C 1s K-edge near edge X-ray absorption fine structure (NEXAFS) spectroscopy for characterizing functional group chemistry of black carbon. *Org. Geochem.* **2011**, *42*, 1055–1064.

